Biochimica et Biophysica Acta 1802 (2010) 1036–1047

Contents lists available at ScienceDirect

Biochimica et Biophysica Acta

journal homepage: www.elsevier.com/locate/bbadis

Methadone induces necrotic-like cell death in SH-SY5Y cells by an impairment of mitochondrial ATP synthesis

Sergio Perez-Alvarez [a], Maria D. Cuenca-Lopez [a], Raquel M. Melero-Fernández de Mera [a], Elena Puerta [b], Andonis Karachitos [c], Piotr Bednarczyk [d], Hanna Kmita [c], Norberto Aguirre [b], Maria F Galindo [e], Joaquin Jordán [a,f,*]

[a] Neuropharmacology, Department of Medical Sciences, College of Medicine, University of Castilla-La Mancha (UCLM), Albacete, Spain
[b] Department of Pharmacology, College of Medicine, Univ. Navarra, Pamplona, Spain
[c] Laboratory of Bioenergetics, Institute of Molecular Biology and Biotechnology, Faculty of Biology, Adam Mickiewicz University, 61-614 Poznan, Umultowska 89, Poland
[d] Department of Biophysics, Warsaw University of Life Sciences-SGGW, Nowoursynowska 159, 02-776 Warsaw, Poland
[e] Translational Neuropsychopharmacology Unit, Albacete University Hospital Center, Albacete, Spain
[f] Institute for Neurologic Disabilities Research, UCLM, Albacete, Spain

ARTICLE INFO

Article history:
Received 27 April 2010
Received in revised form 28 July 2010
Accepted 29 July 2010
Available online 3 August 2010

Keywords:
Methadone
Mitochondria
Necrosis
Neurodegeneration
Bax
Clark electrode

ABSTRACT

Methadone is a widely used therapeutic opioid in narcotic addiction and neuropathic pain syndromes. Oncologists regularly use methadone as a long-lasting analgesic. Recently it has also been proposed as a promising agent in leukemia therapy, especially when conventional therapies are not effective. Nevertheless, numerous reports indicate a negative impact on human cognition with chronic exposure to opiates. Thus, clarification of methadone toxicity is required. In SH-SY5Y cells we found that high concentrations of methadone were required to induce cell death. Methadone-induced cell death seems to be related to necrotic processes rather than typical apoptosis. Cell cultures challenged with methadone presented alterations in mitochondrial outer membrane permeability. A mechanism that involves Bax translocation to the mitochondria was observed, accompanied with cytochrome *c* release. Furthermore, no participation of known protein regulators of apoptosis such as Bcl-X_L and p53 was observed. Interestingly, methadone-induced cell death took place by a caspases-independent pathway; perhaps due to its ability to induce a drastic depletion in cellular ATP levels. Therefore, we studied the effect of methadone on isolated rat liver mitochondria. We observed that methadone caused mitochondrial uncoupling, coinciding with the ionophoric properties of methadone, but did not cause swelling of the organelles. Overall, the effects observed for cells in the presence of supratherapeutic doses of methadone may result from a "bioenergetic crisis." A decreased level of cellular energy may predispose cells to necrotic-like cell death.

The therapeutic opioid methadone (D,L-methadone hydrochloride) is frequently used in different therapies including opioid addiction [1], long-lasting analgesics in cancer and neuropathic pain syndromes [1–3]. Because methadone kills sensitive leukemia cells and breaks chemoresistance and apoptosis resistance in leukemias, it has been proposed as a promising agent in leukemia therapy, especially when conventional therapies are not effective [4]. However, numerous reports indicate a negative impact of chronic exposure to opioid drugs on human cognition. Heroin addicts display a reduction in performance on memory tasks [5,6], correlating with abuse severity [7]. Moreover, patients continuously taking, moderate doses of opioids for chronic pain, and former heroin addicts subjected to methadone maintenance programs also have been reported to show impaired cognitive abilities in psychomotor performance, information processing, attention, problem solving, memory, decision making, and reaction time [7–17]. Thus, research on the toxicity of methadone is required.

Modes of cell demise comprise a number of processes such as apoptosis and necrosis and intermediate options [18]. Calcium (Ca^{2+}) and reactive oxygen species (ROS) have been proposed as second messengers involved in the initial steps of cell death. One of the earliest commitment steps towards cytotoxicity is failure of cytoplasmic Ca^{2+} homeostasis, also known as delayed Ca^{2+} deregulation (DCD). Once DCD is initiated, the process of cell death is irreversible [19–21]. Qualitative, quantitative, and functional changes of mitochondria have been observed, which may cause or strengthen degenerative diseases. Mitochondria-directed cell death stimuli induce a variety of cellular

* Corresponding author. Grupo de Neurofarmacología, Departamento de Ciencias Médicas, Facultad de Medicina, Universidad Castilla-La Mancha, Avda Almansa 14, Albacete-02006, Spain. Tel.: +34 967 599200; fax: +34 967599327.
E-mail address: joaquin.jordan@uclm.es (J. Jordán).

0925-4439/$ – see front matter © 2010 Elsevier B.V. All rights reserved.
doi:10.1016/j.bbadis.2010.07.024

changes, including production of ROS and a marked increase of mitochondrial outer-membrane permeability (MOMP). MOMP will decrease the mitochondrial membrane potential ($\Delta\Psi$) and lead to ATP depletion. Two different routes have been proposed as being mainly responsible for MOMP. First, the formation of mitochondrial permeability transition pores (MPTP), and second, the translocation of pro-apoptotic Bcl-2 family proteins, such as Bax, from the cytosol to the mitochondrial outer membrane [22]. MOMP results in the release of apoptogenic molecules, including cytochrome *c*. These molecules contribute to the formation of the apoptosome, a multimolecular complex that triggers caspase activation. Apoptosome formation is an essential event for cell dismantling through the apoptotic pathway [23]. Since the apoptotic death signalling pathway contains several ATP-dependent steps, the route leading to cell death, apoptosis or necrosis, is determined by the intracellular levels of ATP [24].

The present study was undertaken to characterize the cytotoxic effects of methadone on human SH-SY5Y cells. Our results suggest that methadone induces necrotic-like cell death, since it uncouples mitochondria causing depletion of cellular ATP levels. This, in turn, could be also responsible for caspase-independent cell death, even though we observed mitochondrial cytochrome *c* release, DCD and calpain-protease activation.

1. Materials and methods

1.1. Cell culture and drug treatment procedures

SH-SY5Y cultures were grown as previously described [25] (in Dulbecco's modified Eagle's medium (DMEM) supplemented with 2 mM L-glutamine, penicillin (20 units/mL), streptomycin (5 μg/mL), and 15% (v/v) fetal bovine serum (Gibco, Gaithersburg, MD). Cells were grown in a humidified cell incubator at 37 °C under a 5% CO_2 atmosphere. For GFP-Bax translocation and viability experiments, cells were spotted on μ-Dish 35 mm High IbiTreat (ibidi GmbH, Martinsried, München, Germany) at 2.9×10^5 cells/cm^2 and allowed to attach overnight. Immediately before methadone addition, dilutions of methadone were made and added to fresh cell culture medium. MEF p53−/− cells, a gift from Dr M. Serrano (CNIO, Spain) and SH-SY5Y overexpressing Bcl-X_L (SH-SY5Y-Bcl-X_L) from Dr. J.X. Comella (UAB, Spain), were grown in DMEM supplemented with 2 mM L-glutamine, penicillin (20 units/mL), streptomycin (5 μg/mL), and 15% (v/v) fetal bovine serum.

1.2. Cell viability

For viability experiments, cells were plated at a density of 4×10^4 cells/cm^2 and allowed to attach overnight. Cell viability after methadone additions was assessed by measurement of lactate dehydrogenase activity according to the protocol provided by the manufacturer (Promega). Briefly, the reaction mixture was added to conditioned media and removed from 24-well plate after centrifugation at 250*g* for 10 min. Absorbance of samples at 490 nm was measured in a microplate reader (BioRad, Hercules, CA) after 30 min of incubation at room temperature.

1.3. Transfections

Cells were spotted on μ-Dish 35 mm High IbiTreat 24 h before transfection at a density of 5.3×10^4 cells/cm^2. Cells were transfected with the plasmid GFP-Bax (gift from Prof. Prehn, Dublin, UK)[25]. Transfection was achieved using Lipofectamine reagent (Invitrogen, Carlsbad, CA), according to the manufacturer's protocol. After 4 h of incubation the transfection mixture was removed and replaced with fresh complete medium. At 12 h after transfection, the percentage of cells positive for GFP expression was >70% in each experiment.

1.4. Chromatin state

SH-SY5Y cells were spotted on μ-Dish 35 mm High IbiTreat. After treatment, the glass slides were rinsed three times with PBS and then incubated with 0.5 μg/ml of Hoechst 33342 (Molecular Probes, Inc., Eugene, OR) for 5 min at room temperature. After two rinses with PBS, chromatin staining was analyzed using a fluorescent microscope.

1.5. Caspase activity

After methadone addition, cells were collected in a buffer with the following composition: 25 mM Hepes; 5 mM EDTA; 1 mM EGTA; 5 mM $MgCl_2$; 5 mM DTT; 1 mM PMSF and 10 μg/ml each of pepstatin and leupeptin; pH 7.5. The cellular material was left for 20 min on ice and then sonicated. The lysate was centrifuged for 20 min at 10,000*g* and the supernatant (30 μg protein) was incubated at 37 °C with the fluorogenic substrate DEVD-AFC (15 μM in DMSO, Calbiochem System Products) in a buffer containing 25 mM HEPES (pH 7.5), 10% sucrose, 0.1 CHAPS and 10 mM DTT [26]. Substrate cleavage emitted a fluorescent signal that was quantified in a fluorometer (luminescence-spectrophotometer LS50B, Perkin Elmer, Buckinghamshire, UK) (excitation 400 nm, emission 505 nm). Enzymatic activity is expressed as arbitrary fluorescent units (A.F.U).

1.6. Mitochondrial cytochrome c release

Methadone-treated and control cells were washed once with PBS and collected by centrifugation (2000*g*; 5 min). Cell pellets were resuspended in 200 μl of extraction buffer containing: 250 mM sucrose, 50 mM Tris–HCl, 1 mM EGTA, 1 mM EDTA, 1 mM DTT, 0.1 mM PMSF, pH 7.4; homogenized in a Teflon-glass homogenizer (5 strokes) and, after 15 min on ice, centrifuged (15,000*g*; 15 min). The supernatants (cytosolic fractions) and the pellet (mitochondrial fraction) were separated and analyzed by gel electrophoresis and immunoblotting using anti-cytochrome *c* (1:1000 dilution of rabbit polyclonal IgG, Santa Cruz Biotechnology Inc. CA) [25].

1.7. Cellular ATP concentration

ATP assays were performed using a Sigma luciferin-luciferase assay kit. Controls and methadone-treated cells were resuspended in 1 mL H_2O to disrupt the cell membrane and to quantify the cytosolic ATP. A 10-μl sample was added to 10-μl luciferin–luciferase reaction mix, and immediately the luminescence was read using a luminometer. All values were divided by the protein content (Micro BCA Protein Reagent Kit, Pierce, Rockford, IL), for normalization. Each sample was read three times and the experiment was performed in triplicate.

1.8. Mitochondrial isolation

Rat liver mitochondria were isolated in MSH/EDTA and MSH media containing 210 mM mannitol, 70 mM sucrose, 5 mM Hepes, with or without 1 mM EDTA, pH 7.4, by centrifugal differentiation as described [27]. Mitochondrial protein concentration was measured using the Micro BCA Protein Reagent Kit. The mitochondrial suspensions were kept on ice and immediately used for measurements of oxygen consumption and H_2O_2 production.

1.9. Mitochondrial permeability transition pore activity

Mitochondrial permeability transition pore (MPTP) opening was assayed spectrophotometrically as previously described [28]. In brief, mitochondria were suspended to reach a protein concentration of 1 mg ml^{-1} in 200 μl of solution containing 125 mM KCl, 20 mM

Hepes, 2 mM KH_2PO_4, 1 μM EGTA, 1 mM $MgCl_2$, 5 mM malate and 5 mM glutamate with the pH adjusted to 7.08 with KOH. After addition of different compounds, changes in absorbance at 540 nm (A_{540}), indicating mitochondrial swelling due to MPTP opening, were determined using a microplate reader (BioRad, Hercules, CA). Initial A_{540} values were ~0.8, and minor differences in the loading of the wells were accounted for by representing the data as the fraction of the initial absorbance. Methadone (0.25 or 0.5 mM) was added at the start of the OD measurements which were carried out for 60 min.

1.10. Mitochondrial H_2O_2 generation

The rate of mitochondrial H_2O_2 production was assayed by measuring the increase in fluorescence (excitation at 312 nm, emission at 420 nm) due to oxidation of homovanillic acid by H_2O_2 in the presence of horseradish peroxidase [29]. Reaction conditions were 0.25 mg/ml of mitochondrial protein, 6 U/ml horseradish peroxidase, 0.1 mM homovanillic acid, 50 U/ml superoxide dismutase in the incubation buffer (145 mM KCl, 30 mM Hepes, 5 mM KH_2PO_4, 3 mM $MgCl_2$, 0.1 mM EGTA, 0.1% BSA, pH 7.4) at 37 °C. Methadone was added to mitochondria just before starting the reaction. To start the reaction 2.5 mM glutamate/2.5 mM malate or 5 mM succinate were added as substrates. In some experiments rotenone (2 μM) was included in the reaction mixture to assay maximum rates of complex I and basal complex III H_2O_2 generation. Duplicate samples were incubated for 15 min at 37 °C. The reactions were stopped by transferring the samples to an ice-cold bath and adding 0.5 ml of stop solution (2.0 M glycine, 2.2 M NaOH, 50 mM EDTA, pH 12). Fluorescence was read in a LS50B Perkin-Elmer fluorometer. Known amounts of H_2O_2 generated in parallel by glucose oxidase with glucose as substrate, were used as standards. Since the superoxide dismutase added in excess converts all O_2^- excreted by mitochondria (if any) to H_2O_2, the measurements represent the total ($O_2^- + H_2O_2$) rate of mitROS production.

1.11. Mitochondrial oxygen uptake

The rate of oxygen consumption of isolated liver mitochondria was measured at 37 °C in a water-thermostatized incubation chamber with a computer-controlled Clark-type O_2 electrode (Oxygraph, Hansatech, UK) in 0.5 ml incubation buffer (145 mM KCl, 30 mM Hepes, 5 mM KH_2PO_4, 3 mM $MgCl_2$, 0.1 mM EGTA, 0.1% defatted BSA, pH 7.4). The substrates used were complex I- (2.5 mM glutamate/2.5 mM malate) or complex II-linked (5 mM succinate + 2 μM rotenone). The assays were performed in the absence (state 4-resting state) or in the presence (state 3-phosphorylating state) of 0.5 mM ADP. The total amount of oxygen consumed during state 3 respiration was used for calculating the ADP/O ratio. Different amounts of methadone, in a final volume of 0.2 mL, were added as marked by an arrow in the graphic. Final concentrations in each condition are indicated. Methadone (0.5 mM, if not indicated otherwise) was added during oxygen uptake.

1.12. 3-(4,5-Dimethylthiazol-2-yl)-2,5-diphenyltetrazolium bromide reduction

Reduction of 3-(4,5-dimethylthiazol-2-yl)-2,5-diphenyltetrazolium bromide (MTT) to a blue-colored formazan dye was used to assess the activity of the electron flow along the respiratory chain [30]. Samples of mitochondria (0.1 mg protein) were incubated for 5 min in incubation buffer supplemented with 2.5 mM glutamate/2.5 mM malate in the presence of 0.5 mM methadone or 2 μM rotenone. Then, tubes were warmed to 25 °C in the presence of MTT (0.1 mg/ml) and incubated for another 5 min. Samples were centrifuged and the pellets were resuspended in 1 ml ethanol. Reduction of MTT was measured at 595 nm.

1.13. Integrity of the mitochondrial outer membrane

Determination of the mitochondrial outer membrane integrity was based on the permeability of the membrane to the exogenous cytochrome *c* [31]. Rat liver mitochondria were treated with antimycin A (5 μg/mg) to block the respiratory chain, separated from the cytochrome *c* oxidase segment. Then, 8 mM ascorbate, cytochrome *c* (0.06%) and *N,N,N′,N′*-tetramethyl-1,4-phenylenediamine (TMPD) (in portions of 0.5 mM), were added to get the saturation effect. Methadone (0.5 mM) was added 45 sec prior to antimycin A addition. Respiration rates were calculated using the formula:

$$\frac{\text{cytC} - \text{asc}}{\text{TMPD} - \text{asc}} \times 100\% = I(\%)$$

where I indicates the level of rupture of the outer membrane.

1.14. Conductance measurements in the planar bilayer lipid membrane (BLM)

Membranes were formed from soybean asolectin, suspended at a concentration of 25 mg/mL in n-decane, across a circular hole (aperture diameter about 250 μm) in the thin wall of a Delrin chamber (Warner Instruments) separating two compartments (*cis–trans*). The chamber was connected to recording equipment through a matched pair of Ag-AgCl electrodes. Methadone was added in small aliquots to the *cis* compartment, where also the voltage was held. Both compartments were filled with unbuffered 1 M KCl, pH 7.0 in the presence of a voltage of 10 mV, or with 20 mM Tris buffer of pH, 6.8 in the *cis* compartment and pH 8.8 in the *trans* compartment (pH gradient) or with different concentrations of $CaCl_2$ (pH 7.4), 60 mM in the *cis* compartment and 20 mM in the *trans* compartment (Ca^{2+} gradient). Signals were amplified with a BLM-120 bilayer amplifier (Bio-LOGIC Science Instruments) and computer software was used for data collection. The amount of recorded events for a given set of conditions was 20.

1.15. Western blot analysis

SH-SY5Y cell cultures were washed twice with ice-cold PBS and then collected by mechanical scraping in PBS. The suspension was centrifuged at 16,000*g* for 5 min, and the pellet was resuspended in sample buffer. The protein concentration in each sample was quantified (BCA), and equal amounts of protein (30 μg) were loaded on 10% SDS-PAGE gels. After electrophoresis, proteins were transferred to Immobilon PVDF membranes. Non-specific protein binding was blocked with Blotto [4% w/v non-fat dried milk, 4% bovine serum albumin (Sigma) and 0.1% Tween 20 (Sigma)] in PBS for 1 h. The membranes were incubated overnight at 4 °C with anti-p53 [1:1000 dilution of anti-mouse monoclonal (Pab240) sc-99 Santa Cruz], anti-α-fodrin 1:1000 dilution (MAB1622; Chemicon, Millipore Corporation, Billerica, MA) or anti-alpha-tubulin (1:40.000, from Sigma (St. Louis, MO). After washing with Blotto, the membranes were incubated for 1 h with a secondary antibody (1:5000 dilution of peroxidase-labeled anti-mouse, Promega, Madison, WI) in Blotto. The signal was detected using enhanced chemiluminescence detection (Amersham). Immunoblots were developed by exposure to x-ray films (Eastman-Kodak, Rochester, NY). Band intensities were estimated densitometrically on a GS-800 calibrated densitometer (Biorad One).

1.16. Intracellular calcium concentration

Changes in $[Ca^{2+}]_i$ in SH-SY5Y cells attached to glass coverslips were measured fluorimetrically. Cells were incubated for 45 min at 37 °C in Krebs–Hepes solution (144 mM NaCl, 2 mM $CaCl_2$, 5.9 mM KCl, 1.2 mM $MgCl_2$, 11 mM glucose, 10 mM Hepes/NaOH; pH 7.4) containing 7.0 μM fura-2 AM and 16 μM pluronic F-127 (Invitrogen). Loading with fluorescent dye was stopped by washing the cells with Krebs–Hepes

buffer. Coverslips were then placed in an inverted fluorescence microscope (Nikon Eclipse TE2000-S). Fura-2 was alternatingly excited at 340 and 380 nm using a monochromator; emitted light was transmitted through a 505-nm dichroic mirror and 510 nm emission filter before being detected by a CCD camera. Data were analysed using the Metafluor vs. 2.2 program (Universal Imaging, Downingtown).

1.17. Statistics

When only two means were compared, Student's *t*-test was used. For more than two groups of data, statistical significance was assessed by analysis of variance (ANOVA) and by comparison using Turkey's test. Differences were considered significant at $P<0.05$.

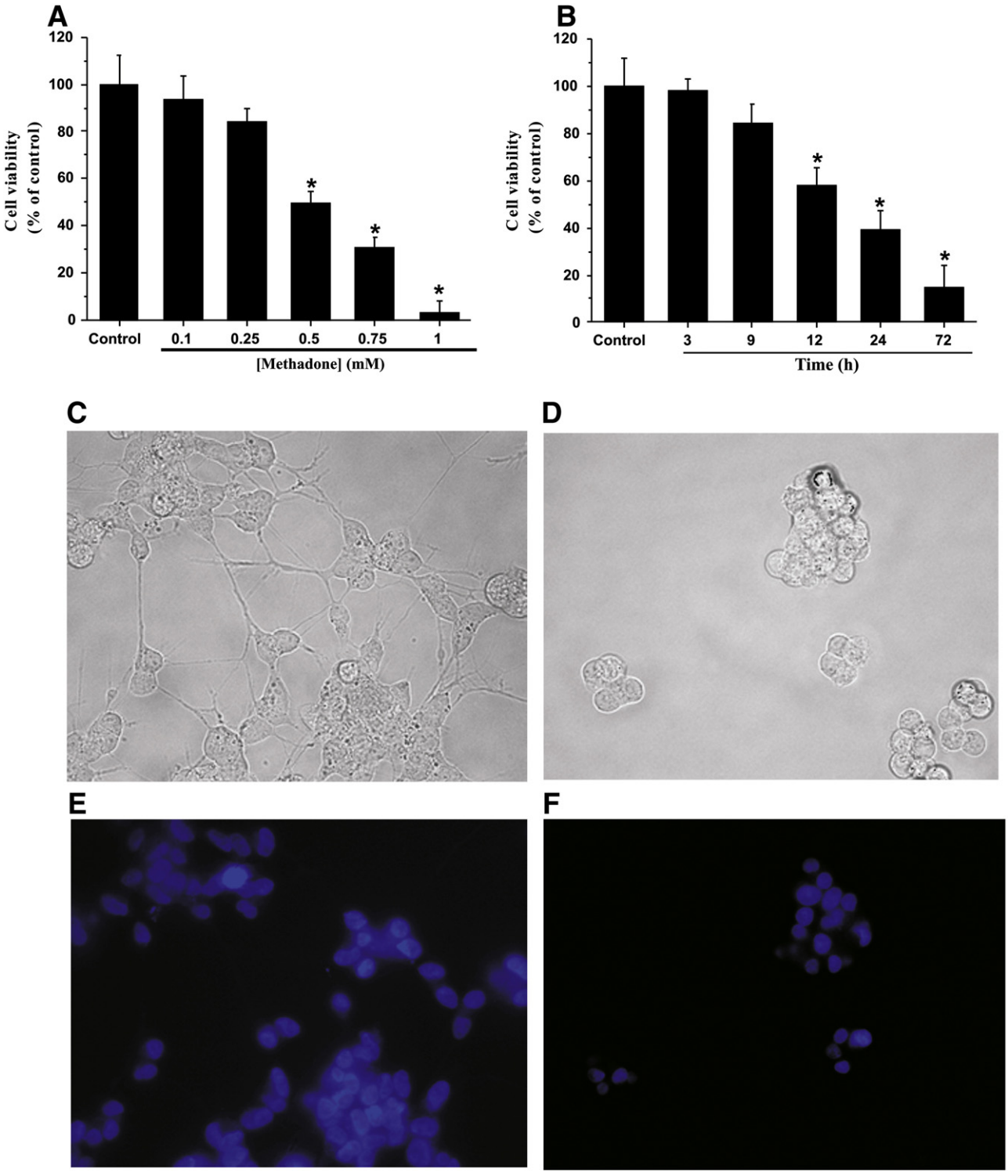

Fig. 1. Methadone induces cell death in SH-SY5Y cell cultures. (A) Cell viability was measured 24 h after methadone addition using LDH release as an indicator of cell death. Data represent mean ± S.E.M. from at least three independent cultures. *$p<0.001$. (B) Time course of cell viability upon 0.5 mM methadone addition to SH-SY5Y cell cultures. Each bar represents the mean ± SEM of 5 different cultures. *$p<0.001$. (C–F) Equal amounts of subconfluent SH-SY5Y cells were incubated with (D and F) or without (C and E) methadone (0.5 mM) for 24 h. (C and D) Phase-contrast microscopy and (E and F) cells stained with Hoechst 33348, examined under an inverted microscope with ultraviolet light (magnification ×63).

2. Results

2.1. Methadone induces necrotic-like cell death in SH-SY5Y cell cultures

Methadone is toxic to different lines cell cultures. In the first set of experiments, we tested the sensitivity of the human neuroblastoma cell line SH-SY5Y to methadone. As shown in Fig. 1A, methadone triggered a concentration- and time-dependent increase in cell death of SH-SY5Y, ranging from 15% to 70% killed cells at a 0.25- to 1.00-mM concentration at 24 h after continuous exposure (Fig. 1A). Methadone treatment at 0.5 mM led to ~40% cell death after 24 h and was used in subsequent experiments. Next, a time-dependent analysis was performed. During the initial 9 h of exposure, minimal changes in viability of the cultures were observed, however significant cell death was detected at later time points (Fig. 1B). Phase-contrast microscopy of SH-SY5Y cells showed a flattened morphology and extended neuritis under control conditions (Fig. 1C), whereas the addition of 0.5 mM methadone induced neurite retraction, absence of cytoplasmic extensions and cell rounding (Fig. 1D). Using dye Hoechst 33348 the chromatin state in cells challenged with methadone was analyzed. Cells with fragmented chromatins were not overrepresented in cultures challenged for 24 h with methadone as compared to the control (Fig. 1E and F). The absence of this hallmark of apoptosis suggests that rather than apoptosis a necrotic-like cell death process might be involved.

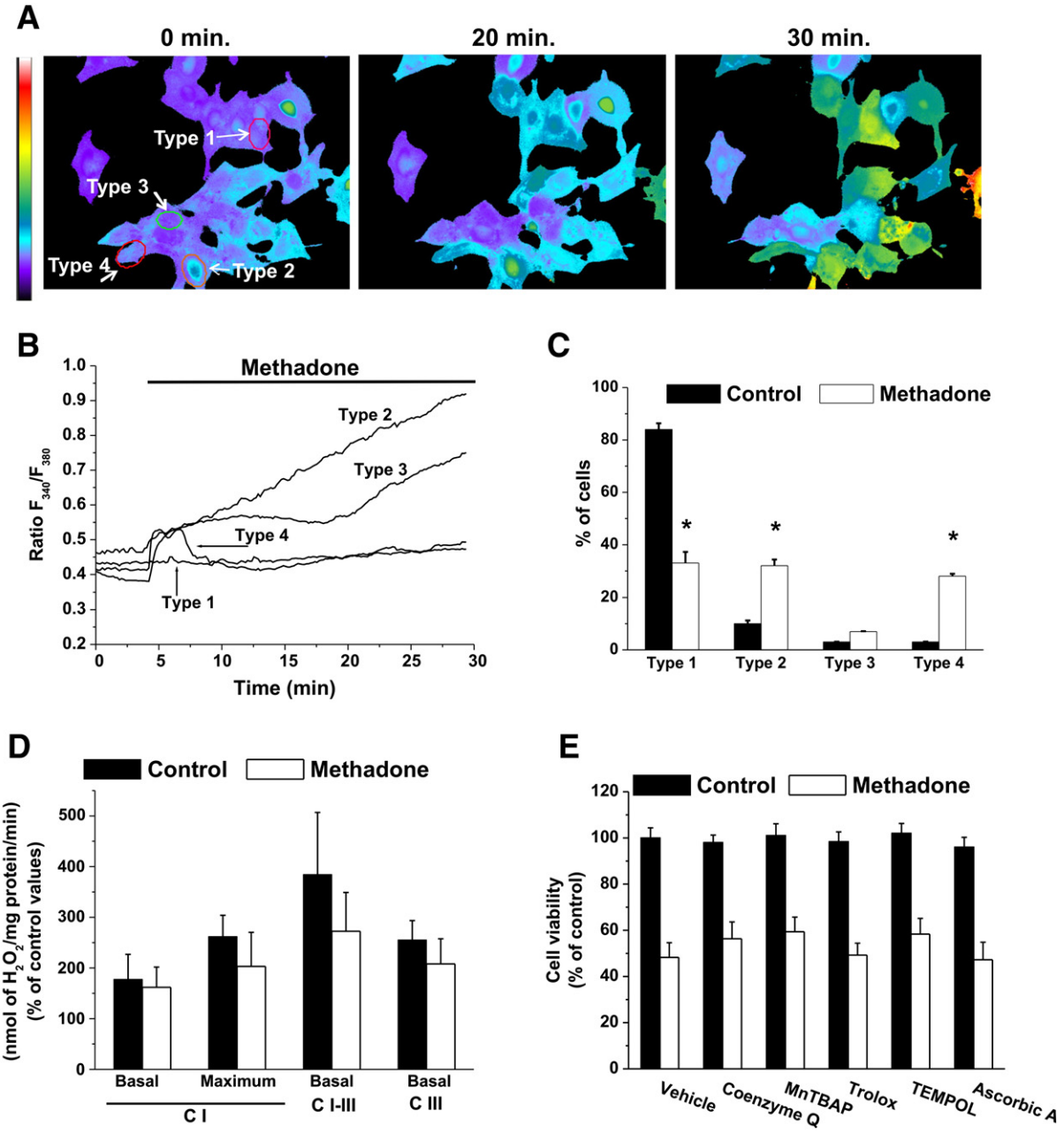

Fig. 2. Methadone induces Ca^{2+} dyshomeostasis. (A–C) $[Ca^{2+}]_i$ in SH-SY5Y cells was measured for 30 min. (B) Representative responses for four different cell types. (C) Fractions of cells that exhibit types 1–4 in $[Ca^{2+}]i$ over time. Data represent those of control (305 cells) or with methadone (258 cells) studied in 18 independent experiments. $^*p<0.001$. (D) Methadone did not induce H_2O_2 production in mitochondria isolated from liver. Histogram illustrates the rates of H_2O_2 production of complex I (C-I), complex I-III (C-I–III) and complex III (C-III) in the presence of methadone. Data shown are mean ± SEM obtained from four independent mitochondrial preparations. (E) Treatment with antioxidant drugs did not prevent methadone-induced cell death. Coenzyme Q (50 μM), MnTBAP (10 μM), Trolox (0.75 mM), TEMPOL (0.2 μM) or ascorbic acid (500 μM) were added 30 min prior to methadone. Cell viability was determined 24 h after methadone addition. Values represent the mean ± SEM of 5 experiments.

To determine whether the observed effects of methadone were transduced through opiate receptors, the effect of naloxone, an opiate receptor antagonist, on methadone-induced SH-SY5Y cell death was determined. Naloxone (10 μM) did not prevent methadone-induced cytotoxic effects (0.5 mM methadone 46.26 ± 5.22 %; methadone + naloxone 41.36 ± 6.36 % cell viability; $n = 5$).

2.2. Methadone induces deregulation of Ca^{2+} but not ROS homeostasis

In the next set of experiments, the possible participation of second messengers such as Ca^{2+} and ROS in methadone-induced cell death was analyzed. SH-SY5Y cells were loaded with fura2/AM to monitor changes in intracellular Ca^{2+} concentrations ($[Ca^{2+}]_{i.}$). Fig. 2A shows images corresponding to $[Ca^{2+}]_i$ during perfusion with and without methadone (0.5 mM) at different time points. Four different cell populations (types 1–4) can be distinguished by their response to methadone (Fig. 2B). About 42% of the cells showed no rise in $[Ca^{2+}]_i$ during the entire $[Ca^{2+}]_i$ measurement period (Type 1; Fig. 2B). Among the remaining cells, we observed cells that were unable to regulate $[Ca^{2+}]_i$ homeostasis shortly upon the addition of methadone (type 2, 22% of the cells) and cells where $[Ca^{2+}]_i$ deregulation takes place with a delay few minutes (type 3, 8.1%). The remaining 26% of the cells were able to control $[Ca^{2+}]_i$ after an initial increase (type 4, Fig. 2C). In the same period, cells not exposed to methadone showed no increase in $[Ca^{2+}]_i$. This intracellular response required the presence of extracellular calcium, because when Ca^{2+} was withdrawn from the extracellular medium, methadone failed to increase intracellular calcium levels ($n = 48$ cells).

To determine if methadone was modifying mitochondrial ROS (mitROS) homeostasis, the rate of mitochondrial H_2O_2 production in isolated mitochondria was measured as the increase in fluorescence due to oxidation of homovanillic acid by H_2O_2. Methadone failed to

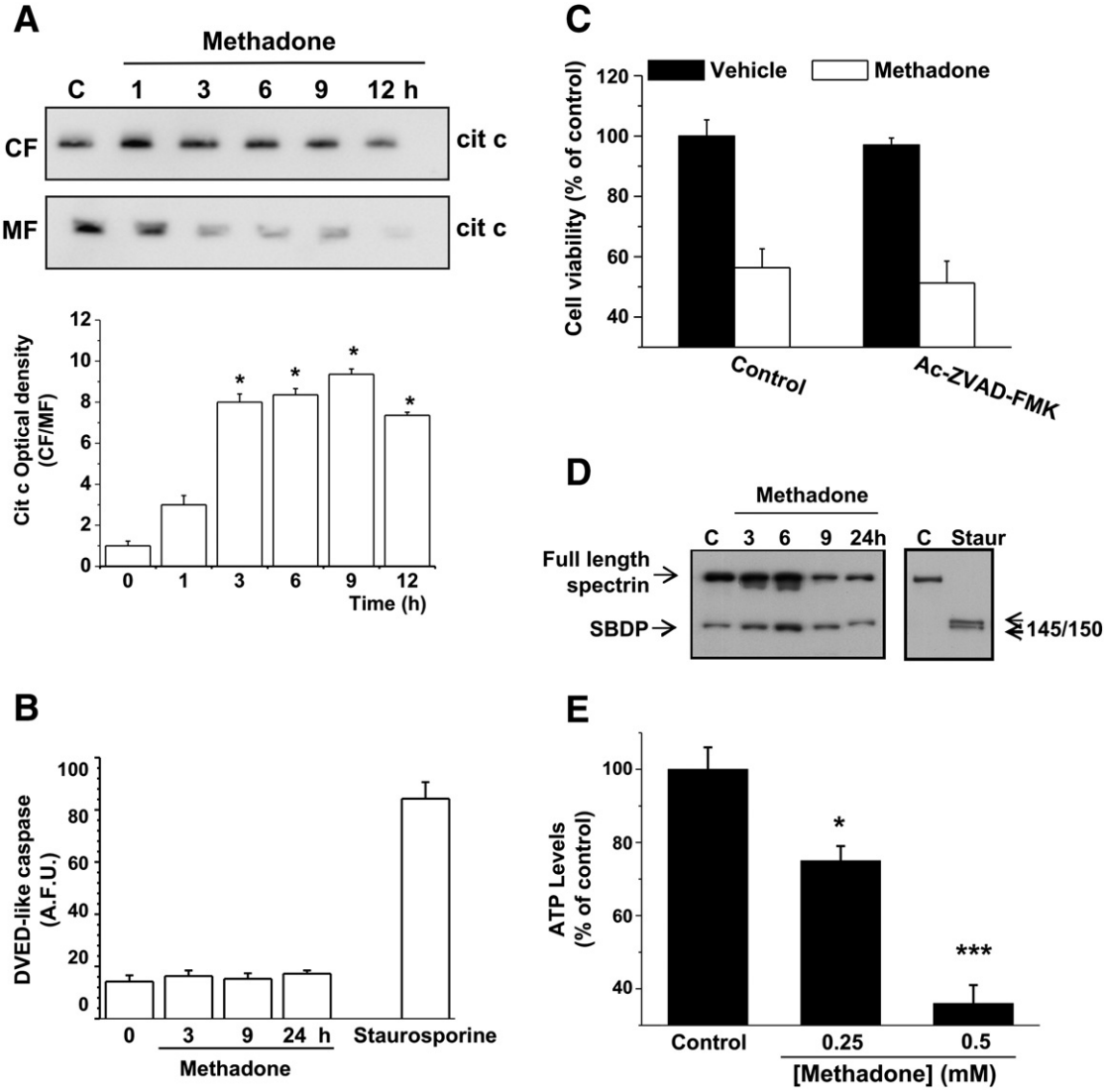

Fig. 3. Methadone induces cytochrome *c* release, but does not activate the caspase-mediated pathway. (A) Methadone induces a time-dependent translocation of cytochrome *c* from the mitochondria to the cytosol. Cytosolic (CF) and mitochondrial (MF) fractions from SH-SY5Y cells challenged with methadone were collected at the indicated times and assayed for cytochrome *c* by immunoblotting. Shown is a representative experiment that was repeated three times with similar results. Histograms represent the relative values of the densitometric analysis. (B) Methadone fails to induce DVED-like caspase activity in SH-SY5Y cells. As a positive control, staurosporine (100 nM, 24 h) treatment markedly increased DVED-like caspase activity. Data represent mean ± SEM of three experiments measured in triplicate. (C) Inhibition of caspase did not block methadone-induced cell death. Cell cultures were incubated with 100 μM Ac-ZVAD-FMK from 30 min prior the addition of methadone until the end of the experiment. Cell viability was determined after 24 h. Data represent mean ± SEM of three independent experiments measured in duplicate. (D) Methadone induced calpain but not caspase signature spectrin breakdown products (SBDP). Immunoblot of total cellular extracts from SH-SY5Y cultures challenged with methadone. Extracts from cells challenged with staurosporine (100 nM, 24 h) were used as a positive control of caspase activation. (E) Methadone induces ATP depletion. Cell cultures were challenged with methadone and 24 h later the ATP levels were determined. ATP levels are expressed relative to control cultures. Data shown are mean ± SEM obtained from three independent cultures. $^{*}P<0.05$; $^{***}P<0.001$.

alter mitROS production at any of the tested concentrations (Fig. 2D). Consistent with this absence of mitROS deregulation by methadone, 30 min pre-treatment with different ROS scavenger drugs such as Coenzyme Q (50 μM), MnTBAP (10 μM), Trolox (0.75 mM), TEMPOL (0.2 μM) or ascorbic acid (500 μM) did not provide cytoprotection to SH-SY5Y cells against methadone-induced toxicity (Fig. 2E).

2.3. Interaction of methadone with the mitochondrial-based apoptotic pathway

The mitochondrion has been proposed to be the headquarters for cell death processes [22]. When the intrinsic or mitochondrial-based cell death pathway is engaged, pro-apoptotic factors such as cytochrome *c* are released from mitochondria with subsequent activation of caspase-3. Release of cytochrome *c* to the cytoplasm was detected in extracts from SH-SY5Y cells following methadone exposure (Fig. 3A). Cytosolic levels of cytochrome *c* began to increase at 3 to 6 h post-treatment. However, no activation of caspase-3 enzymatic activity was found in cellular extracts using DEVD-AFC as a fluororimetric substrate (Fig. 3B). Furthermore, Ac-ZVAD-FMK, a wide-spectrum caspase inhibitor [32], did not abrogate methadone-induced cell death (Fig. 3C). Finally, the activity of caspase-3 was monitored as proteolysis of the cytoskeletal protein alpha-spectrin into spectrin breakdown products (SBDP). Extracts from methadone treated cells showed large increases of 145 kDa calpain-mediated SBDP (up to 3-fold) by 6 h after addition.

One possible explanation for the lack of caspase-3 activation after cytochrome *c* release found in our experiments might be that ATP was depleted due to methadone treatment. To address this issue, ATP levels in cells challenged for 24 h with methadone were measured by the luciferase method. As shown in Fig. 3E, methadone caused depletion of ATP levels in a concentration-dependent way.

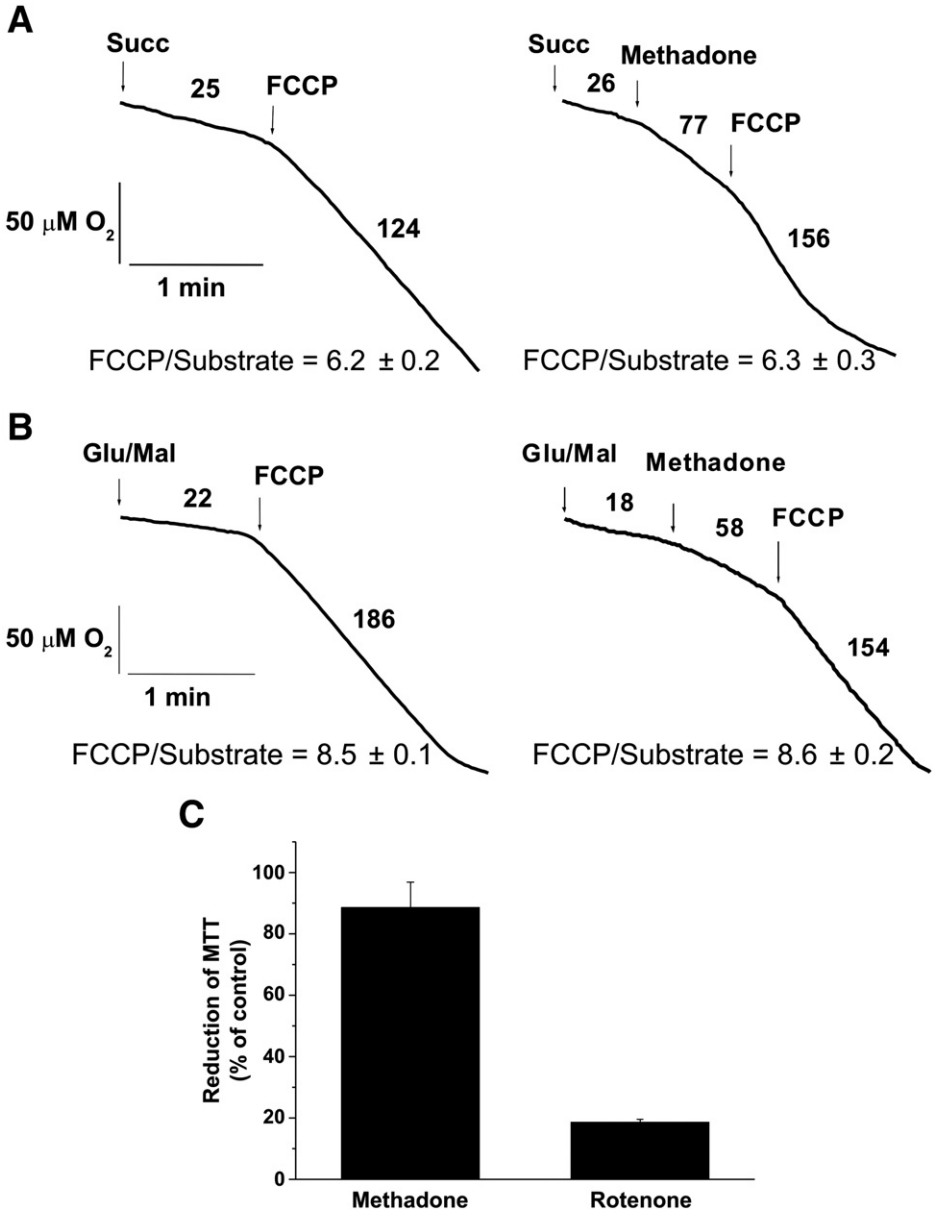

Fig. 4. Effect of methadone on the mitochondrial respiratory chain. (A–B) Influence of 0.5 mM methadone on uncoupled state respiration. Uncoupled state was triggered by 1 μM FCCP in the presence of complex I (2.5 mM glutamate/2.5 mM malate) or complex II (5 mM succinate) dependent respiration. The numbers on the traces refer to respiration rates in nmol oxygen/mg protein/min at 37 °C. Traces shown are the mean obtained from 7 mitochondria preparations. (C) Effect of methadone on electron flow within the respiratory chain. Rotenone, which blocks the transfer of electrons from FeS N-2 centers to ubiquinone, was used as a negative control. Data shown are the mean ± SEM obtained from three independent mitochondria preparations.

2.4. Effect of methadone on mitochondrial respiration

To check if the ATP depletion results from inhibition of the mitochondrial respiratory chain, the effect of methadone on uncoupled state respiration, triggered in isolated mitochondria by FCCP in the presence of complex I or complex II dependent respiration was measured. For this purpose, glutamate/malate and succinate were used as respiratory substrates. Since uncoupled state is the state of maximum capacity of the respiratory chain, the inhibitory effect of methadone could be easily monitored. Independent of the respiratory substrate used, the rate of oxygen uptake in the presence of FCCP relative to the rate of oxygen uptake in the absence of the uncoupler (the FCCP/substrate ratio) did not significantly change in the presence of methadone. Thus, the effect of methadone on mitochondria was not due to inhibition of any of the respiratory chain complexes. Furthermore, in the presence of the synthetic electron acceptor MTT inhibition of electron transfer within the respiratory chain was not observed (Fig. 4C).

To further study changes of mitochondrial activity imposed by methadone, the effect on mitochondrial oxygen uptake coupling to ATP synthesis was measured. Using glutamate/malate and succinate as respiratory substrates, methadone increased the rate of oxygen uptake in state 4 (resting state) in a concentration-dependent manner, and had no effect on state 3 (phosphorylating state, coupled to ATP synthesis) (Fig. 5A–B). The traces obtained for glutamate/malate in the presence of 0.125 and 0.25 mM methadone in a

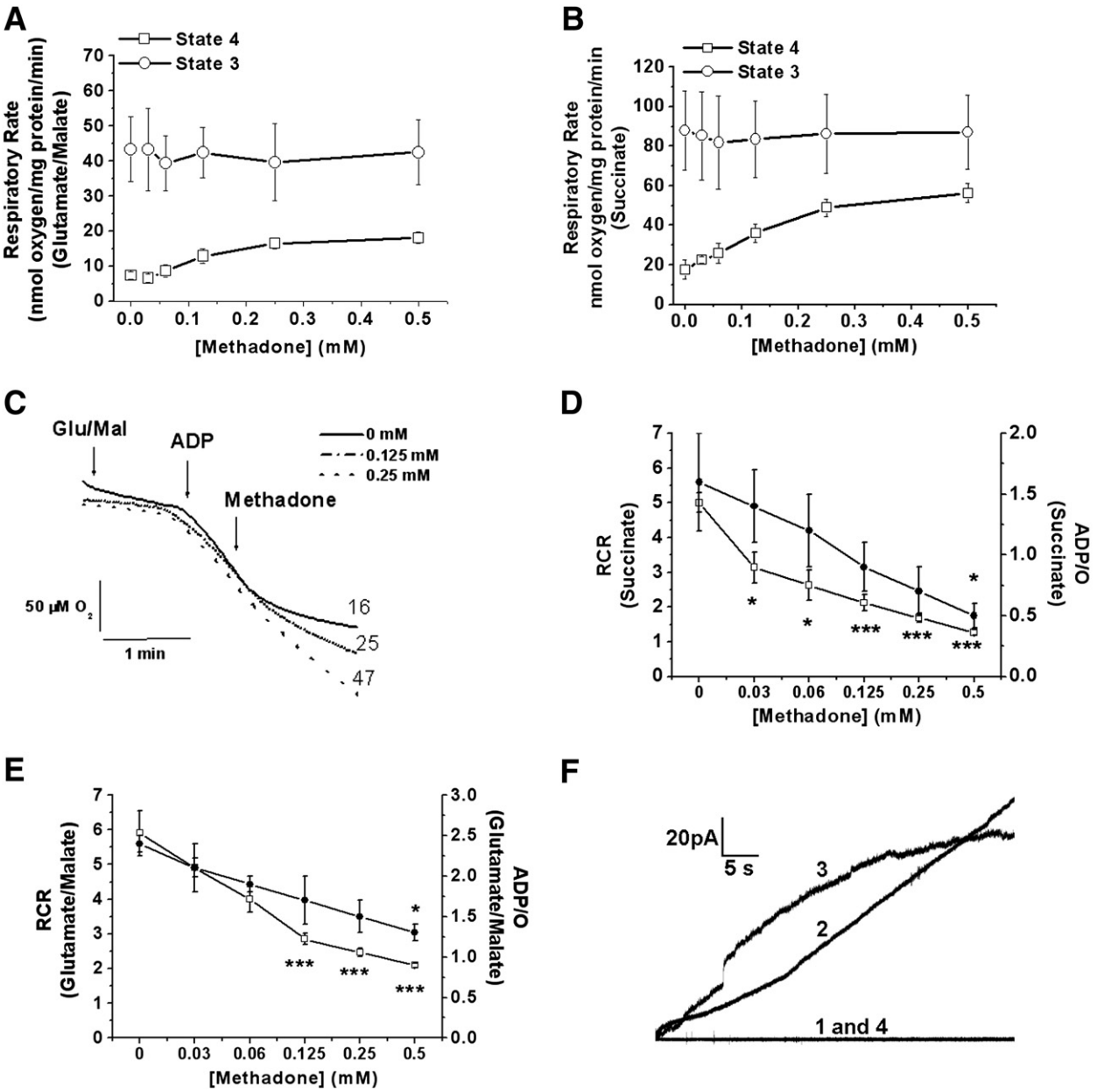

Fig. 5. Effect of methadone on mitochondrial respiration. (A–B) Titrations of state 4 and state 3 respiration with methadone. State 4 was supported by 2.5 mM glutamate/2.5 mM malate (A) or 5 mM succinate (in the presence of 2 µM rotenone) (B). The respiration rate of state 3 was measured in the presence of 500 µM ADP. (C) Traces showing the effect of methadone on state 4 and state 3 respiration obtained for glutamate/malate as a respiratory substrate in the presence of 0.125 mM and 0.25 mM methadone. Traces shown are the mean of six independent mitochondria preparations. Numbers on the traces refer to respiration rates in nmol oxygen/mg protein/min at 37 °C. (D–E) Methadone effect on the calculated values of the RCR (open squares) and ADP/O (solid circles) in the presence of 2.5 mM glutamate/malate (D) or 5 mM succinate (E). *$P<0.05$; ***$P<0.001$. (F) Ion conductivity induced in bilayer lipid membrane by 0.5 mM methadone in the presence of 1 M KCl, proton gradient or Ca^{2+} gradient. The presented events are representative for 20 records obtained for a given set of conditions; 1. control, 2. ΔpH, 3. 1 M KCl, 4. ΔCa^{2+}.

representative experiment are given in Fig. 5C. Methadone, in a concentration-dependent manner, increased the respiratory rate of state 4 but hardly modified the respiratory rate of state 3. As a consequence, the respiratory control ratio (RCR) values calculated for both glutamate/malate and succinate were clearly lowered in the presence of methadone (Fig. 5D–E) suggesting uncoupling. Moreover, methadone also resulted in a delay of return to the resting state 4 leading to a decrease of the ADP/O ratio (Fig. 5D–E), which supports uncoupling. To quantify the effects of methadone on state 4 respiration supported by either glutamate/malate or succinate we calculated the values of $K_{0.5}^{methadone}$, which represents the concentration of methadone resulting in half-maximum of its effect on state 4. The calculated values were 0.126 mM for glutamate/malate and 0.143 mM for succinate. This small difference indicates that the observed effect of methadone was not influenced by the applied respiratory substrate, and probably reflects uncoupling which might result from a possible interaction with phospholipid membranes [33]. To check this possibility a set of experiments using the planar bilayer lipid membrane (BLM) model were performed. As shown in Fig. 5F, in the presence of a proton gradient or KCl methadone induced ion permeability in planar phospholipid membranes indicating that methadone has ionophoric, including protonophoric, properties. However, in the presence of a Ca^{2+} gradient, the permeability is not triggered, which suggests ion selectivity of the methadone effect.

2.5. Bax redistribution, but not MPTP, participates in mitochondrial outer membrane permeabilization changes.

Cytochrome *c* is released from mitochondria as a result of changes in permeabilization of the outer mitochondrial membrane, through different mechanisms such as the formation of MPTP or the translocation of Bax to the mitochondrion. Changes in the absorbance of a mitochondrial suspension at 540 nm can be used to monitor mitochondrial swelling though the activity of MPTP. Methadone failed to induce mitochondrial swelling at any of the concentrations tested (Fig. 6B). Addition of 75 μM $CaCl_2$ was used as control trigger of mitochondrial swelling. To analyse whether methadone pre-disposes mitochondria to Ca-induced swelling, isolated mitochondria were pre-incubated wit methadone for 30 min before Ca^{2+} addition. Under these conditions methadone did not affect Ca-induced swelling (data not show). In addition, the integrity of the mitochondrial outer membrane in isolated mitochondria preparations was assayed by determination of the membrane permeability to exogenous cytochrome *c*. The value of the integrity index (I), which indicates the fraction of mitochondria with the outer membrane disrupted, was 15.4 ± 1.56% in the absence of methadone and 14.7 ± 2.89 ($P>0.05$) in the presence of methadone (Fig. 6B). Moreover, the effects of methadone on mitoplast oxygen uptake were similar to those observed for mitochondria, indicating no effect on the mitochondrial outer membrane (data not shown). We therefore conclude that methadone did not affect the outer membrane.

To determine whether Bax protein was translocated from the cytoplasm to the mitochondria after methadone addition, we transiently overexpressed GFP-Bax in SH-SY5Y cells and visualized the fluorescence pattern after drug treatment [25]. The GFP-Bax fluorescence changed from a diffuse, cytosolic pattern to a punctuated, mitochondrial pattern upon translocation (Fig. 6C, lower panel). Quantification indicated methadone significantly induced Bax translocation to the mitochondria after 12 h of treatment (Fig. 6D).

2.6. Cellular pathways involved in methadone-induced cell death

The induction of certain genes such as p53 has been shown to be a requirement in cell death induced after DNA damage [25,34].

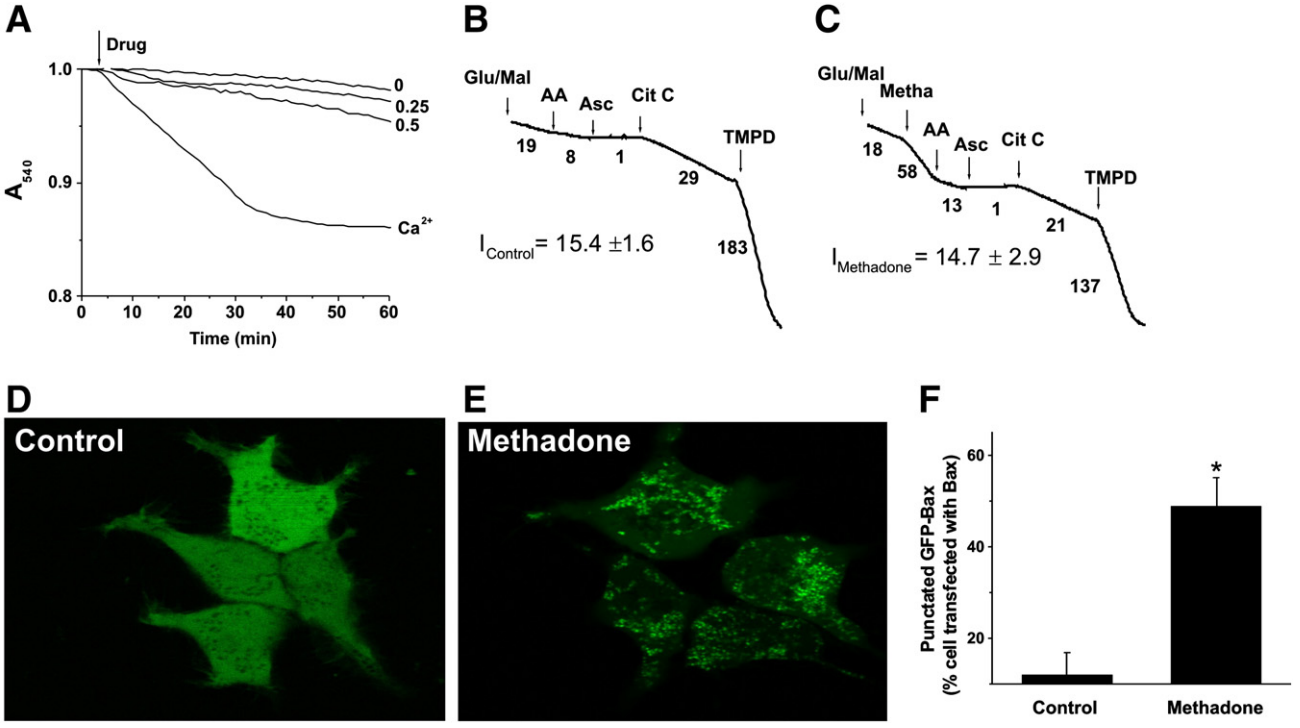

Fig. 6. Methadone induces MOPM trough Bax translocation. (A) Methadone does not induce MPTP formation. Methadone was added (0.25 and 0.5 mM) to isolated mitochondria. Mitochondrial swelling was measured by changes in absorbance at 540 nm. Ca^{2+} was used as a positive control for mitochondrial swelling. Values are the mean from an experiment performed in triplicate. Similar data were obtained with seven different mitochondrial preparations. (B–C) Methadone does not disrupt the outer mitochondrial membrane based on the permeability of the membrane to the exogenous cytochrome *c*. 0.5 mM methadone was added. The values of the integrity index (I) are the mean ± SEM of at least four experiments, each performed in triplicate. (D–E) SH-SY5Y cells were transfected with GFP–Bax, incubated for 24 h to allow for sufficient GFP-Bax expression after which methadone was added. After 12 h of exposure to methadone, the cells were fixed and confocal images were captured. (F) Fraction of cells with punctuate Bax distribution after 12 h of methadone treatment. Values are the mean ± SEM of four experiments, each performed in triplicate. *$P< 0.001$.

Therefore, the effect of methadone on the levels of p53 protein in SH-SY5Y cells was studied. Methadone did not promote the accumulation of p53 protein as compared to untreated cells at any time point assayed (Fig. 7A). Furthermore, the phosphorylation levels of p-53 at serine15 also remained unchanged (Fig. 7A). As expected from these results, methadone-induced cell death was not abrogated, either when p53 activity was inhibited with pifithrin-α (500 nM), or when fibroblast cultures from mice lacking p53 (MEF p53−/−) were used (Fig. 7B).

To further study the mitochondrial-based pathway, the role of the anti-apoptotic protein Bcl-X_L in SH-SY5Y cells challenged with methadone at different time points was analyzed. As shown, the levels of this protein remained unchanged after the addition of methadone (Fig. 7A). Further experiments using SH-SY5Y cells overexpressing Bcl-X_L (SH-SY5Y-Bcl-X_L)[35] revealed that overexpression of this anti-apoptotic protein did not provide any protection against methadone-induced cell death (Fig. 7B).

3. Discussion

This study was aimed at addressing whether an overdose of methadone is related to alterations in cell survival. We demonstrated that high concentrations of methadone promoted death of SH-SY5Y cells, and obtained new evidence that drug abuse may cause death of neuronal cells resulting in irreversible neuronal damage. The pharmacological cause of this effect seems to be related to a depletion of cellular ATP levels by impaired functioning of mitochondria.

Although our experimental observations required high concentrations of methadone to have lethal effects, this study sheds new light on the molecular mechanism underlying the gross impairments that may leads to neuronal damage by chronic drug abuse and opioid addition [36]. Our data also support the high morbidity and mortality associated with opioid dependence. Furthermore, because methadone probably also displays large interindividual variability in its pharmacodynamics, methadone treatment must be adjusted to each patient individually. The high concentration required to induce toxic effects is consistent with previous reports where opioid peptides–synthetic and natural–at a dosage of 10^{-6} M did not influence the growth of the different cell lines studied [37–39]. Other compounds, such a DAMGO, morphine and etorphine caused significant increase in the number of apoptotic cells [37]. Based on experiments with the antagonist naloxone, some of those studies, in agreement with our data, reported that methadone-toxic pathways are not mediated by μ receptors [37,40,41].

The cellular hallmarks analysed here indicate the involvement of a necrotic-like pathway in methadone-induced cell death: first, in cell cultures challenged with methadone, fragmented chromatins were scarce and, second, methadone resulted in a dramatic depletion of ATP. The latter can be responsible for necrotic-like cell death since alterations in cellular energy charge play a major role in the decision of a cell to die by apoptosis or necrosis [42]. Necrosis has been observed in various situations indicating that it is not linked to the toxic effect of a particular condition. In interdigital webs of Apaf-1−/−

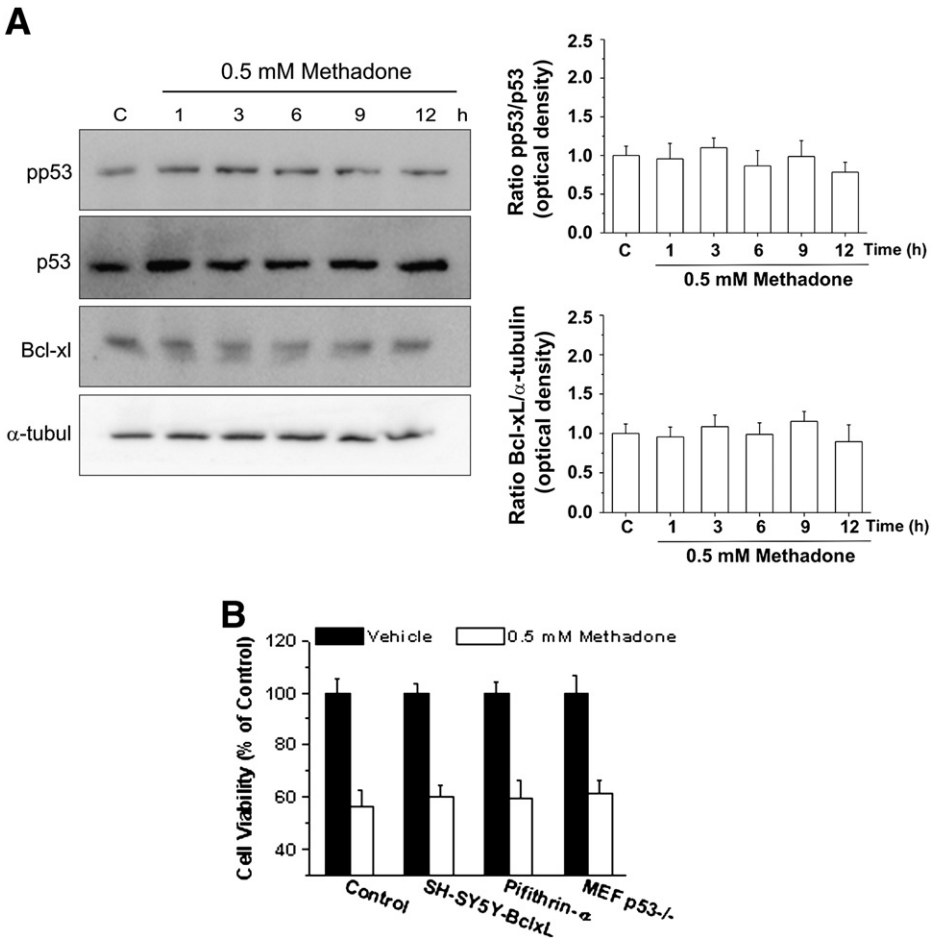

Fig. 7. Methadone does not to activate cellular pathways. (A) Total cellular extracts from SH-SY5Y cells challenged with 0.5 mM methadone were collected at the indicated time-points and assayed by immunoblotting. Shown is a representative experiment that was repeated three times with similar results. Protein loading amount was checked by re-blotting the filters with p53 or anti-α-tubulin antibodies. Histograms represent the relative values from the densitometric analysis. (B) Cell death triggered by methadone is not prevented by the overexpression of Bcl-X_L (SH-SY5Y-Bcl-X_L), by deficiency in p53 (MEF p53−/−) proteins or by pretreatment with pifithrin-α (500 nM, 30 min). Cell death was determined after 24 h of treatment. Values are mean ± SEM of at least three independent experiments.

mice, caspase-independent necrosis occurs as part of development in a programmed, non-accidental manner [43].

Our data indicate that the severe methadone-induced drop in ATP levels is not caused by inhibition of the mitochondrial respiratory chain. Methadone did not inhibit the respiratory chain complexes and it influenced neither the oxygen uptake in uncoupled state nor the electron transfer from the respiratory chain to the synthetic electron acceptor MTT. On the other hand, the results obtained indicate that the observed ATP depletion may consequence from mitochondrial uncoupling. Oxygen uptake measurements showed that methadone increased the respiratory rate of resting state 4 in a concentration-dependent manner. It did not influence the respiratory rate of phosphorylating state 3, although it did cause a delay of return to the resting state 4. As a consequence, methadone decreased the respiratory control ratio (RCR) and the ADP/O ratio. The observed uncoupling effect of methadone did not depend on the applied respiratory substrate as the calculated values of $K_{0.5}^{\text{methadone}}$ for state 4 supported by glutamate/malate and succinate were comparable. Moreover, as shown in BLM model, the uncoupling activity of methadone can be explained by its capability to induce conductivity for small ion in phospholipid membranes. Methadone is a small molecule that contains hydrophilic and hydrophobic parts. Thus, methadone can be regarded as a small and amphipathic molecule, which is consistent with the basic properties of compounds that act in the mitochondria as ionophores. Moreover, it has been shown that methadone, like other opioids (buprenorphine, codeine, dextromethorphan, diprenorphine, etorphine, meperidine, morphine, and naloxone), induces membrane leakage of liposomes composed of phospholipids, and penetrates into monolayers made of phospholipids [33]. Thus, also naloxone appears to act as an ionophore, which could in turn explain why naloxone did not prevent the methadone-induced cytotoxic effect. It is clear that methadone does not selectively affect only the ion permeability of the inner mitochondrial membrane. Nevertheless, the characteristic phospholipid compositions of different cell membranes as well as existing ion gradients may contribute to the ionophoric properties of methadone. Changes in the ion permeability of the inner mitochondrial membrane can be easily monitored. Accordingly, FCCP is known to uncouple mitochondria due to an increase in the permeability of the inner membrane for protons. However, the effect of FCCP was also observed in the BLM model in the presence of a proton gradient but not in the presence of KCl (our unpublished results). Thus, an effect of FCCP on the outer mitochondrial membrane cannot be excluded but is difficult to measure. Thus, the ionophoric properties of methadone might also affect the ion permeability of other cell membranes including the plasma membrane and thereby mediate processes crucial for cell survival, e.g. membrane voltage, intracellular ion concentration, pH and cell volume. Importantly, as shown in the BLM model, methadone is not able to trigger Ca^{2+} movement across phospholipid membranes. Therefore changes in Ca^{2+} homeostasis in the presence of methadone may be caused indirectly via changes in other ion gradients imposed by methadone.

Methadone-induced Ca^{2+} homeostasis deregulation was observed in about 40 % of the cells studied. These cells may have lost their ability to regulate intracellular Ca^{2+} homeostasis. If Ca^{2+} plays a primary role in SH-SY5Y cell death, individual cells with higher Ca^{2+} levels would be predicted to die more rapidly. In fact, SH-SY5Y cells retained cytoplasmic Ca^{2+} indicators after delayed Ca^{2+} deregulation (DCD), indicating that the plasma membrane remains intact for a period of time. One could postulate that once DCD has occurred, these cells are committed to die, as in excitotoxic or hypoxic neuronal injury, which has been interpreted as being causes of cell death [19–21,44].

ROS have been shown to play an important role in cell death after Ca^{2+} increase. Since methadone failed to induce ROS production, our findings suggest that ROS may be the end-products of cytotoxic processes, triggered by a transient Ca^{2+} increase, rather than the cause of DCD. Consistent with this is the general ineffectiveness of antioxidants to decrease DCD in the presence of glutamate [45]. Methadone induced indirect changes in the mitochondrial outer membrane permeability, leading to the release of cytochrome *c* from mitochondria to the cytosol. Apart from uncoupling, this may add to an impairment of ATP synthesis. This was accompanied by the translocation of the pro-apoptotic protein Bax from the cytosol to the mitochondria 12 h after methadone addition but not by swelling of the organelle as a result of opening MPTP. The Bax translocation after methadone treatment was also not accompanied by activation of caspase-3 activity or by the abrogation of the cytotoxic effects of methadone by the caspase inhibitor Ac-ZVAD-FMK. This is consistent with the general idea that apoptosis is an active, energy-requiring process, and with experiments showing that prevention of ATP production inhibits caspase activation in some experimental models [24,46,47]. However, caspase activity is not a requirement for cell death. Indeed, under some circumstances MOMP leads to a complete loss of clonogenic survival, even when executor caspases are inactive [48–51]. Accordingly, caspase-independent necrosis might account in part for the relatively limited extent of abnormalities seen in some caspase-null mutant mice. The results presented here strongly suggest the existence of a caspase-independent cascade of events leading to necrosis, as an alternative to the more classical caspase-dependent cascade leading to apoptosis [43]. In contrast to our results, others have reported that methadone does induce caspase activation and apoptosis in leukaemia cells by activating the intrinsic mitochondrial pathway [4]. These discrepancies might be due to differences in the cell type, experimental model or perhaps the drug concentration used.

Consistent with the idea of necrotic cell death, methadone did not increase the phosphorylation levels of p53, which is involved in cell death processes after DNA damage [34,52]. Our observation fits well with the data from Drummer and colleagues who demonstrated that opioids can induce apoptosis and growth inhibition in human lung cancer cells, despite the presence of mutations in their p53 genes [53]. Furthermore, we found no involvement of anti-apoptotic proteins such as the Bcl-2-like protein Bcl-X_L, which have been proposed to be a part of the defence mechanism against oxidative stress [35,54]. Bcl-X_L might provide a link between cell energy metabolism and apoptosis, and was proposed to prevent apoptosis by facilitating mitochondrial respiration in conditions of poor metabolite supply [55,56]. Although we have shown previously that in Bcl-X_L overproducing cells cytotoxicity is largely reduced [35], these cultures were as sensitive to methadone as wild type cells.

In conclusion, methadone, in supratherapeutic doses, induces necrotic-like cell death in SH-SY5 cells due to its ionophoric properties, which caused a “bioenergetic crisis” and a decrease in the level of cellular energy. This could also explain the toxic effect of methadone observed in different cell types including neurons, cells lines [41], hepatocytes [57], cancer [37] and leukaemia cells [4].

Acknowledgments

This work was supported by grant SAF2008-05143-C03-1 from CICYT: Investigación sobre drogodependiencias. Ministerio de Sanidad y Consumo (04005-00) and PI2007/55 Consejería de Sanidad from Junta de Comunidades de Castilla-La Mancha (to J.J.), by “CCM Obra Social y Cultural-FISCAM” and “Incorporación de grupos emergentes” FIS CARLOS III (to M.F.G.). RM M-F is a fellow FPU. S P-A is a fellow from the Spanish Ministerio de Sanidad y Consumo. Grant SAF2008-05143-C03-2 to NA.

References

[1] M.J. Krantz, P.S. Mehler, Treating opioid dependence. Growing implications for primary care, Arch Intern Med 164 (2004) 277–288.
[2] S. Mercadante, Opioid titration in cancer pain: a critical review, Eur J Pain 11 (2007) 823–830.

[3] S. Mercadante, Methadone in cancer pain, Eur J Pain 1 (1997) 77–83 discussion 84–75.
[4] C. Friesen, M. Roscher, A. Alt, E. Miltner, Methadone, commonly used as maintenance medication for outpatient treatment of opioid dependence, kills leukemia cells and overcomes chemoresistance, Cancer Res 68 (2008) 6059–6064.
[5] C.C. Papageorgiou, I.A. Liappas, E.M. Ventouras, C.C. Nikolaou, E.N. Kitsonas, N.K. Uzunoglu, A.D. Rabavilas, Long-term abstinence syndrome in heroin addicts: indices of P300 alterations associated with a short memory task, Prog Neuropsychopharmacol Biol Psychiatry 28 (2004) 1109–1115.
[6] D. Guerra, A. Sole, J. Cami, A. Tobena, Neuropsychological performance in opiate addicts after rapid detoxification, Drug Alcohol Depend 20 (1987) 261–270.
[7] A. Verdejo, I. Toribio, C. Orozco, K.L. Puente, M. Perez-Garcia, Neuropsychological functioning in methadone maintenance patients versus abstinent heroin abusers, Drug Alcohol Depend 78 (2005) 283–288.
[8] E.R. Gritz, S.M. Shiffman, M.E. Jarvik, J. Haber, A.M. Dymond, R. Coger, V. Charuvastra, J. Schlesinger, Physiological and psychological effects of methadone in man, Arch Gen Psychiatry 32 (1975) 237–242.
[9] S. Darke, J. Sims, S. McDonald, W. Wickes, Cognitive impairment among methadone maintenance patients, Addiction 95 (2000) 687–695.
[10] M. Specka, T. Finkbeiner, E. Lodemann, K. Leifert, J. Kluwig, M. Gastpar, Cognitive-motor performance of methadone-maintained patients, Eur Addict Res 6 (2000) 8–19.
[11] H.V. Curran, J. Kleckham, J. Bearn, J. Strang, S. Wanigaratne, Effects of methadone on cognition, mood and craving in detoxifying opiate addicts: a dose-response study, Psychopharmacology (Berl) 154 (2001) 153–160.
[12] C. Kornreich, M.L. Foisy, P. Philippot, B. Dan, J. Tecco, X. Noel, U. Hess, I. Pelc, P. Verbanck, Impaired emotional facial expression recognition in alcoholics, opiate dependence subjects, methadone maintained subjects and mixed alcohol-opiate antecedents subjects compared with normal controls, Psychiatry Res 119 (2003) 251–260.
[13] M.Z. Mintzer, M.L. Stitzer, Cognitive impairment in methadone maintenance patients, Drug Alcohol Depend 67 (2002) 41–51.
[14] E. Bruera, K. Macmillan, J. Hanson, R.N. MacDonald, The cognitive effects of the administration of narcotic analgesics in patients with cancer pain, Pain 39 (1989) 13–16.
[15] A. Vainio, J. Ollila, E. Matikainen, P. Rosenberg, E. Kalso, Driving ability in cancer patients receiving long-term morphine analgesia, Lancet 346 (1995) 667–670.
[16] T. Galski, J.B. Williams, H.T. Ehle, Effects of opioids on driving ability, J Pain Symptom Manage 19 (2000) 200–208.
[17] J.A. Haythornthwaite, L.A. Menefee, A.L. Quatrano-Piacentini, M. Pappagallo, Outcome of chronic opioid therapy for non-cancer pain, J Pain Symptom Manage 15 (1998) 185–194.
[18] M. Leist, M. Jaattela, Four deaths and a funeral: from caspases to alternative mechanisms, Nat Rev Mol Cell Biol 2 (2001) 589–598.
[19] M. Tymianski, M.P. Charlton, P.L. Carlen, C.H. Tator, Source specificity of early calcium neurotoxicity in cultured embryonic spinal neurons, J Neurosci 13 (1993) 2085–2104.
[20] H. Manev, M. Favaron, A. Guidotti, E. Costa, Delayed increase of Ca2+ influx elicited by glutamate: role in neuronal death, Mol Pharmacol 36 (1989) 106–112.
[21] R.D. Randall, S.A. Thayer, Glutamate-induced calcium transient triggers delayed calcium overload and neurotoxicity in rat hippocampal neurons, J Neurosci 12 (1992) 1882–1895.
[22] J. Jordan, V. Cena, J.H. Prehn, Mitochondrial control of neuron death and its role in neurodegenerative disorders, J Physiol Biochem 59 (2003) 129–141.
[23] C. Brenner, G. Kroemer, Apoptosis. Mitochondria—the death signal integrators, Science 289 (2000) 1150–1151.
[24] Y. Eguchi, S. Shimizu, Y. Tsujimoto, Intracellular ATP levels determine cell death fate by apoptosis or necrosis, Cancer Res 57 (1997) 1835–1840.
[25] M. Gomez-Lazaro, M.F. Galindo, C.G. Concannon, M.F. Segura, F.J. Fernandez-Gomez, N. Llecha, J.X. Comella, J.H. Prehn, J. Jordan, 6-Hydroxydopamine activates the mitochondrial apoptosis pathway through p38 MAPK-mediated, p53-independent activation of Bax and PUMA, J Neurochem 104 (2008) 1599–1612.
[26] J. Jordan, M.F. Galindo, R.J. Miller, Role of calpain- and interleukin-1 beta converting enzyme-like proteases in the beta-amyloid-induced death of rat hippocampal neurons in culture, J Neurochem 68 (1997) 1612–1621.
[27] H.R. Lotscher, K.H. Winterhalter, E. Carafoli, C. Richter, Hydroperoxide-induced loss of pyridine nucleotides and release of calcium from rat liver mitochondria, J Biol Chem 255 (1980) 9325–9330.
[28] B.S. Kristal, P.N. Staats, A.I. Shestopalov, Biochemical characterization of the mitochondrial permeability transition in isolated forebrain mitochondria, Dev Neurosci 22 (2000) 376–383.
[29] A. Sanz, P. Caro, J. Gomez, G. Barja, Testing the vicious cycle theory of mitochondrial ROS production: effects of H2O2 and cumene hydroperoxide treatment on heart mitochondria, J Bioenerg Biomembr 38 (2006) 121–127.
[30] Y. Liu, D.A. Peterson, H. Kimura, D. Schubert, Mechanism of cellular 3-(4, 5-dimethylthiazol-2-yl)-2, 5-diphenyltetrazolium bromide (MTT) reduction, J Neurochem 69 (1997) 581–593.
[31] R. Douce, R. Bourguignon, R. Brouquisse, M. Neuberger, Isolation of plant mitochondria: General principles and criteria of integrity, Meth Enzymol 148 (1987) 403–415.
[32] M. Garcia-Calvo, E.P. Peterson, B. Leiting, R. Ruel, D.W. Nicholson, N.A. Thornberry, Inhibition of human caspases by peptide-based and macromolecular inhibitors, J Biol Chem 273 (1998) 32608–32613.
[33] F. Reig, M.A. Busquets, I. Haro, F. Rabanal, M.A. Alsina, Interaction of opiate molecules with lipid monolayers and liposomes, J Pharm Sci 81 (1992) 546–550.
[34] M. Gomez-Lazaro, M.F. Galindo, F.J. Fernandez-Gomez, J.H. Prehn, J. Jordan, Activation of p53 and the pro-apoptotic p53 target gene PUMA during depolarization-induced apoptosis of chromaffin cells, Exp Neurol 196 (2005) 96–103.
[35] J. Jordan, M.F. Galindo, D. Tornero, C. Gonzalez-Garcia, V. Cena, Bcl-x L blocks mitochondrial multiple conductance channel activation and inhibits 6-OHDA-induced death in SH-SY5Y cells, J Neurochem 89 (2004) 124–133.
[36] E.J. Nestler, Under siege: The brain on opiates, Neuron 16 (1996) 897–900.
[37] I.S. Zagon, P.J. McLaughlin, Opioids and the apoptotic pathway in human cancer cells, Neuropeptides 37 (2003) 79–88.
[38] I.S. Zagon, J.P. Smith, R. Conter, P.J. McLaughlin, Identification and characterization of opioid growth factor receptor in human pancreatic adenocarcinoma, Int J Mol Med 5 (2000) 77–84.
[39] P.J. McLaughlin, R.J. Levin, I.S. Zagon, Regulation of human head and neck squamous cell carcinoma growth in tissue culture by opioid growth factor, Int J Oncol 14 (1999) 991–998.
[40] X.H. Ren, J. Zhao, L. Pu, K. Ling, D.L. Yin, G. Pei, Differential neurotoxicity of etorphine-like opiates: lack of correlation with their ability to activate opiate receptors, Toxicon 36 (1998) 735–743.
[41] D.L. Yin, X.H. Ren, Z.L. Zheng, L. Pu, L.Z. Jiang, L. Ma, G. Pei, Etorphine inhibits cell growth and induces apoptosis in SK-N-SH cells: involvement of pertussis toxin-sensitive G proteins, Neurosci Res 29 (1997) 121–127.
[42] C. Richter, M. Schweizer, A. Cossarizza, C. Franceschi, Control of apoptosis by the cellular ATP level, FEBS Lett 378 (1996) 107–110.
[43] M. Chautan, G. Chazal, F. Cecconi, P. Gruss, P. Golstein, Interdigital cell death can occur through a necrotic and caspase-independent pathway, Curr Biol 9 (1999) 967–970.
[44] F.W. Marcoux, A.W. Probert Jr., M.L. Weber, Hypoxic neuronal injury in tissue culture is associated with delayed calcium accumulation, Stroke 21 (1990) III71-74.
[45] O. Vergun, A.I. Sobolevsky, M.V. Yelshansky, J. Keelan, B.I. Khodorov, M.R. Duchen, Exploration of the role of reactive oxygen species in glutamate neurotoxicity in rat hippocampal neurones in culture, J Physiol 531 (2001) 147–163.
[46] M. Latta, G. Kunstle, M. Leist, A. Wendel, Metabolic depletion of ATP by fructose inversely controls CD95- and tumor necrosis factor receptor 1-mediated hepatic apoptosis, J Exp Med 191 (2000) 1975–1985.
[47] D. Ferrari, A. Stepczynska, M. Los, S. Wesselborg, K. Schulze-Osthoff, Differential regulation and ATP requirement for caspase-8 and caspase-3 activation during CD95- and anticancer drug-induced apoptosis, J Exp Med 188 (1998) 979–984.
[48] J. Xiang, D.T. Chao, S.J. Korsmeyer, BAX-induced cell death may not require interleukin 1 beta-converting enzyme-like proteases, Proc Natl Acad Sci USA 93 (1996) 14559–14563.
[49] G.P. Amarante-Mendes, D.M. Finucane, S.J. Martin, T.G. Cotter, G.S. Salvesen, D.R. Green, Anti-apoptotic oncogenes prevent caspase-dependent and independent commitment for cell death, Cell Death Differ 5 (1998) 298–306.
[50] V.S. Marsden, T. Kaufmann, A. O'Reilly, L.J.M. Adams, A. Strasser, Apaf-1 and caspase-9 are required for cytokine withdrawal-induced apoptosis of mast cells but dispensable for their functional and clonogenic death, Blood 107 (2006) 1872–1877.
[51] M.F. Galindo, J. Jordan, C. Gonzalez-Garcia, V. Cena, Chromaffin cell death induced by 6-hydroxydopamine is independent of mitochondrial swelling and caspase activation, J Neurochem 84 (2003) 1066–1073.
[52] M. Gomez-Lazaro, F.J. Fernandez-Gomez, J. Jordan, p53: twenty five years understanding the mechanism of genome protection, J Physiol Biochem 60 (2004) 287–307.
[53] R. Maneckjee, J.D. Minna, Opioids induce while nicotine suppresses apoptosis in human lung cancer cells, Cell Growth Differ 5 (1994) 1033–1040.
[54] F.J. Fernandez-Gomez, M.F. Galindo, M. Gomez-Lazaro, V.J. Yuste, J.X. Comella, N. Aguirre, J. Jordan, Malonate induces cell death via mitochondrial potential collapse and delayed swelling through an ROS-dependent pathway, Br J Pharmacol 144 (2005) 528–537.
[55] E. Gottlieb, M.G. Vander Heiden, C.B. Thompson, Bcl-x(L) prevents the initial decrease in mitochondrial membrane potential and subsequent reactive oxygen species production during tumor necrosis factor alpha-induced apoptosis, Mol Cell Biol 20 (2000) 5680–5689.
[56] D.S. McClintock, M.T. Santore, V.Y. Lee, J. Brunelle, G.R. Budinger, W.X. Zong, C.B. Thompson, N. Hay, N.S. Chandel, Bcl-2 family members and functional electron transport chain regulate oxygen deprivation-induced cell death, Mol Cell Biol 22 (2002) 94–104.
[57] O.H. Drummer, K. Opeskin, M. Syrjanen, S.M. Cordner, Methadone toxicity causing death in ten subjects starting on a methadone maintenance program, Am J Forensic Med Pathol 13 (1992) 346–350.